Mechano-activated Objects with Multidirectional Shape Morphing Programmed via 3D Printing

Jitkanya Wong,[†] Amrita Basu,[†] Maximilian Wende,[†,§] Nicholas Boechler,[,‡] Alshakim Nelson*[,†]*

[†]Department of Chemistry, University of Washington, Seattle, Washington 98195, United States

[‡]Department of Mechanical and Aerospace Engineering, University of California, San Diego, La Jolla, California 92093, United States

ABSTRACT Mechano-activation as a stimuli-response in 4D printing offers advantages such as orthogonality to other stimuli and control over the magnitude of applied force. Herein, we demonstrate mechanically activated morphing with directional control that is dictated by the patterns produced via multi-material 3D printing. An advantage of this approach is that pre-stretching of the sample is not required. We developed on gel inks comprised of a cross-linkable self-assembling triblock copolymer and polymerizable ionic liquids that varied in the size of the cation. The multi-material printing of these inks afforded objects that changed their shape in a predetermined manner upon the application of a tensile force.

KEYWORDS 4D printing, 3D printing, mechano-activation, stimuli-responsive materials, shape morphing, ion gels, direct-ink write

Stimuli-responsive 3D printed objects (4D printing) have recently garnered much attention due to their potential in the development of robotic actuators, sensors, and biomedical devices.[1–3] By utilizing responsive materials, the printed constructs undergo chemical or physical changes through time when exposure to various stimuli, including temperature, light, or electromagnetic fields, are used to induce a mechanical shape change.[4–8] In contrast, biological systems, such as Venus fly traps and mimosa plants, have inspired a growing interest in 4D objects that respond to mechanical stimuli (either applied force or deformation) to achieve a complex autonomous response.[9–16]

Mechanical forces can be orthogonal to other stimuli and offer facile control over the magnitude of the applied force. One mechanism that has been shown to achieve shape morphing is to leverage composite (e.g. two materials bonded together, which we also refer to as a "bilayer") elements with mismatched elastic properties.[17–21] Upon compressive loading[17] or relaxation of a previously applied strain (e.g. pre-strain)[18–21], composite elements can undergo 3D shape changes via buckling instabilities or bending. Within the context of 4D printing, previously demonstrated examples of mechanically induced shape change have been restricted to 3D printing on already pre-strained layers. The major downside of this approach is that it significantly confines the possible designs that can be printed and the resulting morphed shapes achieved, due to the necessity of a pre-stretched sheet. For instance, prior studies on pre-stretched sheets were restricted to unidirectional folding.[18] Without the need for pre-straining the sample, the ability to easily fabricate complex 3D geometries with multiple materials, can be leveraged, and more complex 4D objects and responses achieved. So far, two examples that demonstrated mechano-activated shape change in the absence of a pre-stretched layer were

achieved by mismatched recovery introduced by alignment of embedded fibers[22] and degree of crystallinity[23], however, these examples cannot be 3D printed, which limits the complexity of their potential shape changes.

Herein, we demonstrate 3D printable ion gel inks that enable fabrication of multi-layered and multi-material objects with tunable viscoelastic and plastic responses, and then show how these inks can be used to create 3D constructs that can undergo multidirectional mechano-activated shape change without the need for pre-strain (Figure 1a). Tailoring the underlying materials' viscoelastic and plastic response enables control over the temporal response of the composite, as well as its reversibility. Shear-thinning ion gel inks based on self-assembling F127-bisurethane methacrylate (F127-BUM, Figure 1b) in imidazolium ionic liquids were previously shown to be effective for direct ink write (DIW) 3D printing to afford robust multi-layered constructs.[24] Unlike hydrogels (a commonly utilized 4D printing ink), ion gels utilize ionic liquids with low vapor pressures[25–27], and as a consequence, do not dry out under ambient conditions. The ionic liquids used to form the ion gels in this study contain vinyl groups that can undergo photo-initiated polymerization (Figure 1c). Thus, after the ion gels were printed, the entire construct was photo-cured to form continuous polymer networks that had varied elastic, viscous, and plastic mechanical proper-ties. Used in the context of multi-material DIW printing, these ion gels with varied mechanical properties enabled our creation of objects that are programmed via 3D printing to undergo multidirectional mechano-activated shape change in response to tensile forces.

Herein, three ion gel inks using polymerizable ionic liquids were developed, which were comprised of F127-BUM dissolved in 1-ethyl-3-vinylimidazolium tetrafluoroborate ([EVIM]BF_4), 1-butyl-3-vinylimidazolium tetrafluoroborate ([BVIM]BF_4), or 1-hexyl-3-

vinylimidazolium tetrafluoroborate ([HVIM]BF_4). The imidazolium ionic liquids possess vinyl groups that can undergo photo-initiated radical polymerization that can also co-polymerize with the methacrylate endgroups of F127-BUM to form a crosslinked polymerized ionic liquid (PIL) network (Figure 1d). Three different alkyl chain lengths were chosen as we hypothesized that these side chains would affect the viscoelastic and plastic properties of both the ion gel and the polymerized ionic liquid. Ion gels that were formed from [EVIM]BF_4 and [BVIM]BF_4 each required 27 wt% F127-BUM to achieve self-supporting gels. SAXS characterization of these ion gels showed multiple distinct signal peaks, which suggested the presence of F127-BUM micelles arranged in an ordered packing structure. The normalized q-value ratios were 1, 1.42, 1.73, roughly corresponding to 1, $1^{1/2}$, $3^{1/2}$, indicating a BCC arrangement, which is consistent with F127-based hydrogels that have been reported in the literature (Supporting Information).[28,29] A higher loading of F127-BUM (37 wt%) was required when [HVIM]BF_4 was the solvent, which was likely due to the increased compatibility between the imidazolium cation and poly(propylene oxide) blocks of the triblock copolymer.

To confirm good shear-thinning behavior during the printing process, rheometrical characterizations were performed on the ion gels. Oscillatory strain-sweep experiments (Figure 2a) displayed the gel-sol transition the ion gels experienced when extruded (at 11% oscillatory strain), and cyclic strain experiments (Figure S6, Supporting Information) showed that the gel-sol transition is fast and reversible over multiple cycles without significant hysteresis. The prior two properties are important in the printing process, as the gel must be able to flow through the nozzle then quickly recover its gel state after exiting the nozzle, and the transition should happen reproducibly each time pressure is applied. Lastly, viscosity vs. shear rate experiments (Figure S7, Supporting Information) showed the decreasing viscosity with increasing shear rate,

confirming that the ion gels are shear-thinning. Additionally, thermogravimetric analysis and electrochemical impedance spectroscopy experiments were performed that show the ion gels retained the ionic conductivity and thermal stability of the ionic liquids (summarized in the Supporting Information).

The ion gels were formulated with a photo radical generator (2-hydroxyl-2-methylpropriophenone, 0.2 wt%), and printed using a pneumatic DIW system. Multi-layered constructs were successfully printed with an extruded filament diameter of ~0.4-0.6 mm (0.26 mm I.D. nozzle, 0.3 mm layer height), and did not require photo-curing between layer deposition. All structures were printed with 0.3 mm layer height. The [EVIM]BF_4 and [BVIM]BF_4 ion gels afforded successful multi-layered objects up to 20 layers, and the viscoelastic properties of the printed ion gel supported overhanging features. The softer [HVIM]BF_4 ion gel afforded constructs containing up to 8 layers with good layer-to-layer integrity (Figure 2b).

All multi-layered constructs were UV-cured after they were entirely printed to encourage isotropic mechanical properties. A single post-print UV-cure reduces the interlayer defects, which is a common source of mechanical weakness in structures printed via 3D printing. Dogbone samples of each ion gel were casted in a mold and 3D printed in two different directions, and then characterized via tensile tests as is shown in Figure 2c. As can be seen in Fig. 2c, the cured [EVIM]BF_4 PIL exhibits the stiffest response, with an elastic modulus of approximately 550 MPa, whereas the polymerized [BVIM]BF_4 and [HVIM]BF_4 PILs were almost an order of magnitude less stiff, with elastic moduli of 68 and 34 MPa, respectively. All three polymers exhibited a highly ductile response, wherein the [EVIM]BF_4 PIL showed the lowest ultimate strain, followed by the [HVIM]BF_4 then [BVIM]BF_4 PILs (see also Table S6,

Supporting Information). The differences in quasi-static mechanical properties between the different elastomers can be explained based on the size of the cation's alkyl side chain length. The [HVIM]BF_4 PIL, having the longest alkyl group of the set, consequently had the lowest T_g and thus the greatest amount of material flexibility.[30] We also observed that the mechanical properties of the PILs were independent of the method of dogbone fabrication (Figure 2c), specifically, whether they were printed vertically, horizontally, or cast in a mold.

The tensile experiments further revealed that all of the PILs exhibited a varied time dependent (and generally nonlinear viscoelastic) recovery toward their original shape, as can be seen in Fig. 2d and e. All three polymers showed an initial, relatively rapid, partial shape recovery from 150% strain within the first 10 seconds, with the [EVIM]BF_4 and [BVIM]BF_4 PILs returning to 100% strain and the [HVIM]BF_4 PIL to 55% strain. After this initial rapid recovery, the viscoelastic recovery becomes slower and more varied between the three samples. After 120 hours, the [EVIM]BF_4 PIL, which exhibits the slowest recovery, retains approximately 54% strain, which suggests a partially plastic response. In contrast, the [BVIM]BF_4 and [HVIM]BF_4 PILs exhibited nearly full shape recovery after 2 hours, with the [HVIM]BF_4 PIL showing the faster recovery. While [EVIM]BF_4, [BVIM]BF_4, and [HVIM]BF_4 polymerized to form linear chains, the F127-BUM serves as a crosslinker in this polymer network and provides the 'memory' of the original shape of the object. We suggest the variable time-dependent recovery is likely due to the transient charge interactions between PIL chains. The larger butyl and hexyl groups can shield the cation, which leads to higher mobility of the chains. The gel fraction for the three different ion gel compositions were all approximately 90%, and the presence of the residual unpolymerized ionic liquid in the PIL is hypothesized to act as a plasticizer. Upon removal of residual ionic liquid, all of the samples showed increased elastic

moduli and decreased ultimate strain, while maintaining a generally ductile response (Supporting Information, Figure S8).

The differences in mechanical properties of the cured ion gel was utilized to print bilayers that were programmed via 3D printing to undergo mechano-activated shape changes. For example, a bilayer construct comprised of a [BVIM]BF_4 PIL layer printed onto a [EVIM]BF_4 PIL layer was cured and then mechano-activated by stretching (150% strain) and releasing the film. The combination of the plastic deformation of the [EVIM]BF_4 PIL layer and the viscoelastic recovery of the [BVIM]BF_4 PIL led to permanent bending of the bilayer construct in the direction of the elastomeric layer. The extent of curvature was dependent upon the applied strain, wherein smaller bending angles were produced with small strains (50%) and larger bending angles at higher strains (100% strain) (Figure 3a, other material combinations are in Supporting Information, Figure S9).

The multi-material DIW printing process also enables the programming of more complex mechano-activated multidirectional shape-morphing. For example, we printed alternating parallel lines of [EVIM]BF_4 and [BVIM]BF_4 ion gels at a 135° angle on top of a [BVIM]BF_4 ion gel layer. The bilayer was UV-cured and then mechano-activated to fold into a helical structure, as is shown in Figure 3b. Bilayers were also programmed via 3D printing to encode letters that were revealed upon mechano-activation (Figure 3c). A “U”, which requires bending in one direction was created by printing [BVIM]BF_4 ion gel on the upper layer in the region where the bend was desired. On the other hand, a “W” required the spatial localization of the [BVIM]BF_4 ion gel within both layers, in different locations, in order to facilitate the bending in opposite directions. Strain-concentrating regions were incorporated into the design in this case to maximize the strain

incurred to the intended bending region, and minimize the strain incurred to the intended straight regions, under application uniaxial tensile load at the edges of the sample.

In summary, we have used multi-material DIW, enabled by polymerizable ion gels, to program the mechano-activated multidirectional folding of planar structures into 3D shapes. The polymerizable ion gels that were developed for this application exhibited variable viscoelastic or viscoelastic-plastic behaviors upon the application and release of a tensile load. The ability to control the viscoelastic and plastic response of the constituent materials of the printed morphing structure offers significant potential benefit, wherein future, time-dependent, sequential folding or autonomous origami schemes can be envisioned. The ion gels exhibited good shear-thinning behavior with rapid transitions between the gel- and sol-states. Mechanical characterization performed on cured structures confirmed minimal interlayer defects were introduced during the printing process. The ionic liquid within the ion gel was polymerized during a post-print UV cure, which led to objects with a high degree of isotropy. Unlike other methods of producing objects that undergo mechanically induced shape changes, our approach does not require pre-stretching before or during fabrication. Thus, the full capabilities of 3D printing can now be used to program more complex geometrical changes upon mechano-activation.

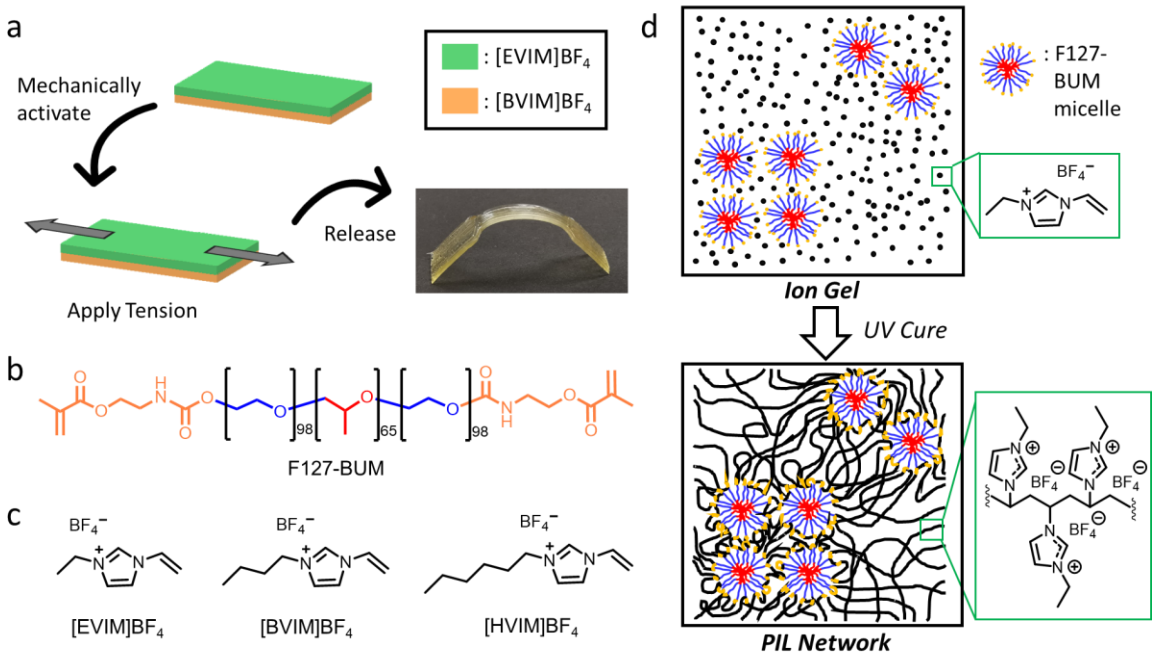

Figure 1. Strategy towards shape change and chemical compositions of the materials. a) Upon stretching and releasing the bilayer, the shape memory materials recover at different rates and to different degrees, allowing the bilayer to bend towards the side that recovers the most. The ion gels used to fabricate these structures were comprised of (b) an F127-based triblock copolymer with bisurethane methacrylate chain ends (F127-BUM) and (c) one of the following ILs: 1-ethyl-3-vinylimidazolium tetrafluoroborate ([EVIM]BF_4), 1-butyl-3-vinylimidazolium tetrafluoroborate ([BVIM]BF_4), or 1-hexyl-3-vinylimidazolium tetrafluoroborate ([HVIM]BF_4). d) The ion gel was shear-thinning and comprised F127-BUM micelles dispersed in the IL. After UV cure (365 nm), the methacrylate chain ends of F127-BUM and IL co-polymerize to form a shape memory polymeric network.

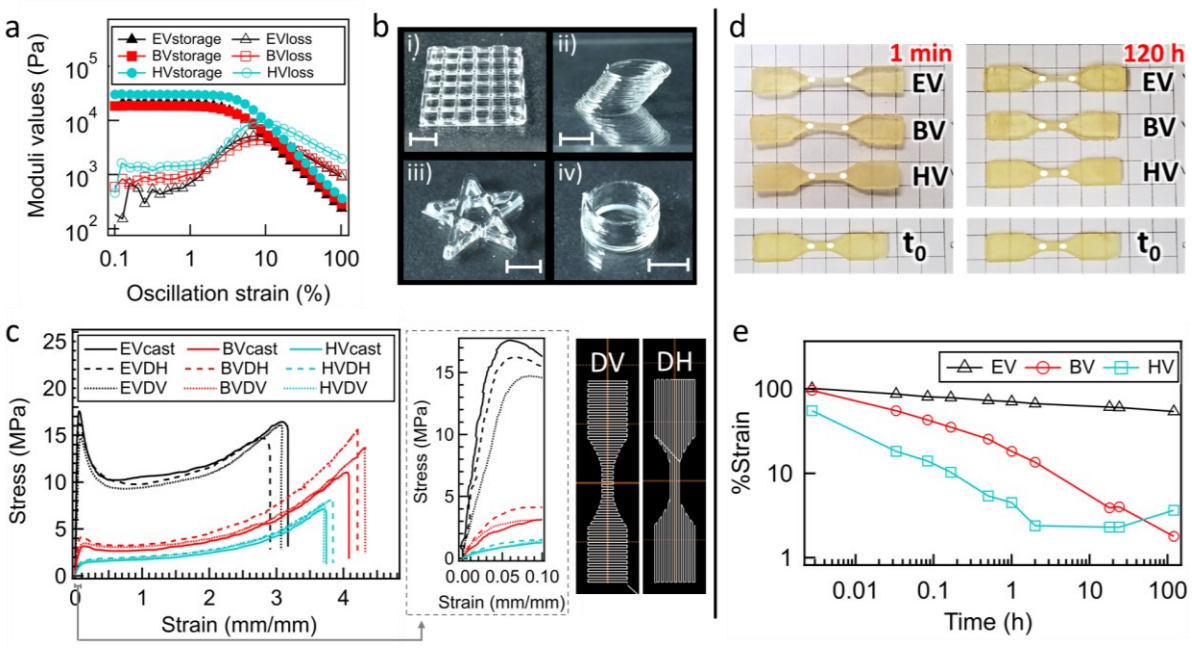

Figure 2. Mechanical characterization of the uncured ion gels and post-cured samples. (a) Oscillatory strain sweep experiment on the ion gels showing the storage and loss moduli as a function of strain. At higher strain, the loss moduli is greater than the storage moduli, suggesting the gel-sol transition that enables printing. (b) Example prints including (scale bar = 5 mm) (i) a 2-layer perpendicular serpentine structure ([EVIM]BF_4 ion gel), (ii) a 20-layer offset cylinder with a 40° overhang ([BVIM]BF_4 ion gel), (iii) an 8-layer 5-pointed star, and (iv) a 20-layer straight cylinder ([HVIM]BF_4 ion gel). c) Stress-strain curves of the cured materials are shown for dogbone samples that were casted, printed perpendicular (DH), or printed parallel (DV) to the axis of applied strain. d) To observe the shape recovery of the cured structures, casted dogbones were stretched to 150% strain and released. e) Shape recovery as a function of time for the ion gels (measured at the dogbones' narrow sections).

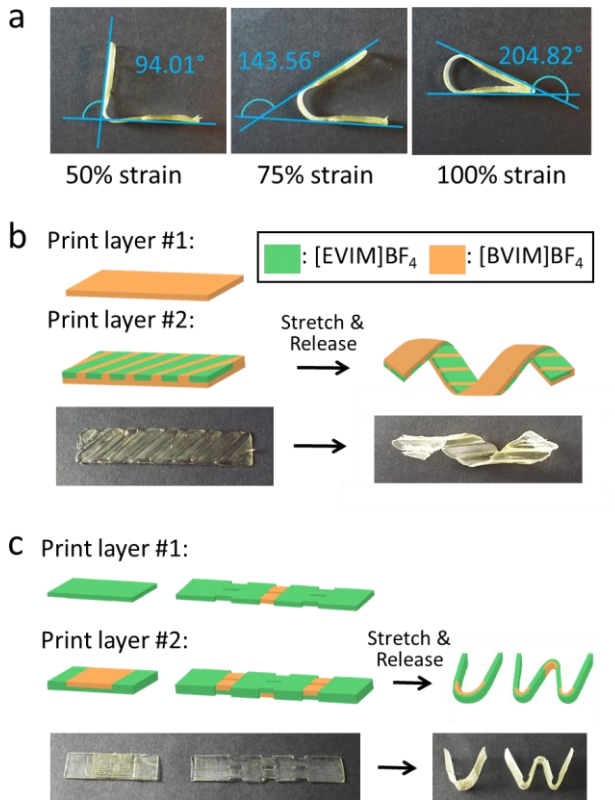

Figure 3. Mechano-activated shape transformations in printed multi-material structures. a) Printed bilayer strips were stretched to different strains, wherein the bending angle is dependent upon the magnitude of applied strain. Mechano-activated shape transformation into (b) a helical ribbon, and (c) planar constructs that were encoded to transform into a “U” and a “W”.

ASSOCIATED CONTENT

The Supporting Information is available free of charge at http://pubs.acs.org

Experimental procedures, ^{1}H and ^{13}C-NMR characterization, ATR-FTIR characterization, small-angle x-ray scattering, rheology, thermogravimetric analysis, electrochemical impedance spectroscopy, tensile test data. (PDF)

Video of real-time bending of printed spoon upon stretch and release. (MP4)

AUTHOR INFORMATION

Corresponding Author

*,‡Email: nboechler@eng.ucsd.edu

*,†Email: alshakim@uw.edu

ORCID

Jitkanya Wong: 0000-0003-1151-2004

Amrita Basu: 0000-0001-6639-9921

Nicholas Boechler: 0000-0001-9639-1533

Alshakim Nelson: 0000-0001-8060-8611

Present Addresses

§Fraunhofer-Institut für Verfahrenstechnik und Verpackung IVV, Verfahrensentwicklung Polymer-Recycling, Giggenhauser Str. 35, Freising, DE 85354, Germany.

Author Contributions

J.W., A.B., N.B., and A.N. conceived the project and designed the overall experiments. J.W. designed the individual experiments. M. W. collected tensile test data. J.W. performed and collected data for the remaining experiments. J.W., M.W., and N.B. analyzed data. J. W., N. B., and A.N. wrote the manuscript, and all authors edited the manuscript. All authors have given approval to the final version of the manuscript.

Funding Sources

We gratefully acknowledge support from the U.S. Army Research Office (W911NF-17-1-0595) for this work. A.N. also acknowledges the National Science Foundation (1752972) for additional support.

Notes

The authors declare no competing financial interest.

ACKNOWLEDGMENT

We thank Dean Waldow for assistance with EIS data analysis, and thank Kristin Schmidt and Chenhui Zhu for assistance with SAXS experiment performed at ALS beamline 7.3.3. This research used resources of the Advanced Light Source, a U.S. DOE Office of Science User Facility under contract no. DE-AC02-05CH11231.

ABBREVIATIONS

DIW, direct-ink-write; [EVIM]BF_4, 1-ethyl-3-methylimidazolium tetrafluoroborate; [BVIM]BF_4, 1-butyl-3-methylimidazolium tetrafluoroborate; [HVIM]BF_4, 1-hexyl-3-methylimidazolium tetrafluoroborate PIL, polymerized ionic liquid.

REFERENCES

(1) Kuang, X.; Roach, D. J.; Wu, J.; Hamel, C. M.; Ding, Z.; Wang, T.; Dunn, M. L.; Qi, H. J. Advances in 4D Printing: Materials and Applications. *Adv. Funct. Mater.* **2019**, *29*, 1805290.

(2) Zhang, Z.; Demir, K. G.; Gu, G. X. Developments in 4D-printing: a review on current smart materials, technologies, and applications. *Int. J. Smart Nano. Mater.* **2019**, *3*, 205–224.

(3) Joshi, S.; Rawat, K.; Karunakaran, C.; Rajamohan, V.; Mathew, A. T.; Koziol, K.; Thakur, V. K.; Balan, A.S.S. 4D printing of materials for the future: Opportunities and challenges. *Applied Materials Today* **2020**, *18*, 100490.

(4) Peng, B.; Yang, Y.; Gu, K.; Amis, E. J.; Cavicchi, K. A. Digital Light Processing 3D Printing of Triple Shape Memory Polymer for Sequential Shape Shifting. *ACS Materials Lett.* **2019**, *1*, 410–417.

(5) Wang, Z. J.; Hong, W.; Wu, Z. L.; Zheng, Q. Site-Specific Pre-Swelling-Directed Morphing Structures of Patterned Hydrogels. *Angew. Chem. Int. Ed.* **2017**, *56*, 15974–15978.

(6) Pezzulla, M.; Shillig, S. A.;Nardinocchia, P.; Holmes. Morphing of geometric composites via residual swelling. *Soft Matter* **2015**, *11*, 5812−5820.

(7) Davidson, E. C.; Kotikian, A.; Li, S.; Aizenberg, J.; Lewis, J. A. 3D Printable and Reconfigurable Liquid Crystal Elastomers with Light-Induced Shape Memory via Dynamic Bond Exchange. *Adv. Mater.* **2020**, *32*, 1905682.

(8) Kim, Y.; Yuk, H.; Zhao, R.; Chester, S. A.; Zhao, X. Printing ferromagnetic domains for untethered fast-transforming soft materials. *Nature* **2018**, *558*, 274–279.

(9) Wang, L.; Zhou, W.; Tang, Q.; Yang, H.; Zhou, Q.; Zhang, X. Rhodamine-Functionalized Mechanochromic and Mechanofluorescent Hydrogels with Enhanced Mechanoresponsive Sensitivity. *Polymers* **2018**, *10*, 994.

(10) Barbee, M. H.; Mondal, K.; Deng, J. Z.; Bharambe, V.; Neumann, T. V.; Adams, J. J.; Boechler, N.; Dickey, M. D.; Craig, S. L. Mechanochromic Stretchable Electronics. *ACS Appl. Mater. Interfaces* **2018**, *10*, 29918−29924.

(11) Meira, R. M.; Correia, D. M.; Ribeiro, S.; Costa, P.; Gomes, A. C.; Gama, F. M.; Lanceros-Méndez, S.; Ribeiro, C. Ionic-Liquid-Based Electroactive Polymer Composites for Muscle Tissue Engineering. *ACS Appl. Polym. Mater.* **2019**, *1*, 2649−2658.

(12) Hu, X.; Zeng, T.; Husic, C. C.; Robb, M. J. Mechanically Triggered Small Molecule Release from a Masked Furfuryl Carbonate. *J. Am. Chem. Soc.* **2019**, *141*, 15018−15023.

(13) Mohanraj, B.; Duan, G.; Peredo, A.; Kim, M.; Tu, F.; Lee, D.; Dodge,G. R.; Mauck, R. L. Mechanically Activated Microcapsules for "On-Demand" Drug Delivery in Dynamically Loaded Musculoskeletal Tissues. *Adv. Funct. Mater.* **2019**, *29*, 1807909.

(14) Diesendruck, C. E.; Steinberg, B. D.; Sugai, N.; Silberstein, M. N.; Sottos, N. R.; White, S. R.; Braun, P. V.; Moore, J. S. Proton-Coupled Mechanochemical Transduction: A Mechanogenerated Acid. *J. Am. Chem. Soc.* **2012**, *134*, 12446−12449.

(15) Rohde, R. C.; Basu, A.; Okello, L. B.; Barbee, M. H.; Zhang, Y.; Velev, O. D.; Nelson, A.; Craig, S. L. Mechanochromic composite elastomers for additive manufacturing and low strain mechanophore activation. *Polym. Chem.* **2019**, *10*, 5985–5991.

(16) Peterson, G. I.; Larsen, M. B.; Ganter, M. A.; Storti, D. W.; Boydston, A. J. 3D-Printed Mechanochromic Materials. *ACS Appl. Mater. Interfaces* **2015**, *7*, 577−583.

(17) Stafford, C. M.; Harrison, C.; Beers, K. L.; Karim, A.; Amis, E. J.; Vanlandingham, M. R.; Kim, H. C.; Volksen, W.; Miller, R. D.; Simonyi, E. E. A buckling-based metrology for measuring the elastic moduli of polymeric thin films. *Nat. Mater.* **2009**, *3*, 545−550.

(18) Cafferty, B. J.; Campbell, V. E.; Rothemund, P.; Preston, D. J.; Ainla, A.; Fulleringer, N.; Diaz, A. C.; Fuentes, A. E.;Sameoto, D.; Lewis, J. A.; Whitesides, G. M. Fabricating 3D Structures by Combining 2D Printing and Relaxation of Strain. *Adv. Mater. Technol.* **2019**, *4*, 1800299.

(19) Yin, L.; Kumar, R.; Karajic, A.; Xie, L.; You, J.; Joshuia, D.; Lopez, C. S.; Miller, J.; Wang, J. From All-Printed 2D Patterns to Free-Standing 3D Structures: Controlled Buckling and Selective Bonding. *Adv. Mater. Technol.* **2018**, *3*, 1800013.

(20) Huang, J.; Liu, A.; Kroll, B.; Bertoldi, K.; Clarke, D. R. Spontaneous and deterministic three-dimensional curling of pre-strained elastomeric bi-strips. *Soft Matter* **2012**, *8*, 6291−6300.

(21) Al-Rashed, R.; Jiménez, F. L.; Marthelot, J.; Reis, P. M. Buckling patterns in biaxially pre-stretched bilayer shells: wrinkles, creases, folds and fracture-like ridges. *Soft Matter* **2017**, *13*, 7969–7978.

(22) Robertson, J. M.; Torbati, A. H.; Rodriguez, E. D.; Mao, Y.; Baker, R. M.; Qi, J.; Mather, P. T. Mechanically programmed shape change in laminated elastomeric composites. *Soft Matter* **2015**, *11*, 5754−5764.

(23) Wisinger, C. E.; Maynarda, L. A.; Barone, J. R. Bending, curling, and twisting in polymeric bilayers. *Soft Matter* **2019**, *15*, 4541−4547.

(24) Wong, J.; Gong, A. T.; Defnet, P. A.; Meabe, L.; Beauchamp, B.; Sweet, R. M.; Sardon, H.; Cobb, C. L.; Nelson, A. 3D Printing Ionogel Auxetic Frameworks for Stretchable Sensors. *Adv. Mater. Technol.* **2019**, *4*, 1900452.

(25) Bideau, J. L.; Viau, L.; Vioux, A. Ionogels, ionic liquid based hybrid materials. *Chem. Soc. Rev.* **2011**, *40*, 907−925.

(26) Ueki, T.; Watanabe, M. Polymers in Ionic Liquids: Dawn of Neoteric Solvents and Innovative Materials. *Bull. Chem. Soc. Jpn.* **2012**, *85*, 33−50.

(27) Marr, P. C.; Marr, A. C. Ionic liquid gel materials: applications in green and sustainable chemistry. *Green Chem.* **2016**, *18*, 105−128.

(28) Mortensen, K.; Batsberg, W.; Hvidt, S. Effects of PEO-PPO Diblock Impurities on the Cubic Structure of Aqueous PEO-PPO-PEO Pluronics Micelles: fcc and bcc Ordered Structures in F127. *Macromolecules* **2008**, *41*, 1720–1727.

(29) Liu, T.; Chu, B. Formation of homogeneous gel-like phases by mixed triblock copolymer micelles in aqueous solution: FCC to BCC phase transition. *J. Appl. Cryst*. **2000**, *33*, 727–730.

(30) Salas-de la Cruz, D.; Green, M. D.; Ye, Y.; Elabd, Y. A.; Long, T. E.; Winey, K. I. Correlating Backbone-to-backbone Distance to Ionic Conductivity in Amorphous Polymerized Ionic Liquids. *J. Polym. Sci. Pol. Phys.* **2012**, *50*, 338–346.